# On the Capacity and Normalisation of ISI Channels

Wei Xiang, *Student Member, IEEE,* and Steven S. Pietrobon, *Senior Member, IEEE*

***Abstract*— We investigate the capacity of various ISI channels with additive white Gaussian noise. Previous papers showed a minimum $E_b/N_0$ of $-4.6$ dB, 3 dB below the capacity of a flat channel, is obtained using the water-pouring capacity formulas for the $1+D$ channel. However, these papers did not take into account that the channel power gain can be greater than unity when water-pouring is used. We present a generic power normalization method of the channel frequency response, namely peak bandwidth normalisation, to facilitate the fair capacity comparison of various ISI channels. Three types of ISI channel, *i.e.*, adder channels, RC channels and magnetic recording channels, are examined. By using our channel power gain normalization, the capacity curves of these ISI channels are shown.**

***Index Terms*— Capacity, Normalisation, ISI.**

## I. Introduction

CALCULATING the capacity of various ISI channels has been an interesting research topic for some time. For calculation of the channel capacity, the unit energy impulse response of the channel (unit energy normalisation) is commonly used. For a flat channel, the transmit power to the receive power ratio is unity when using unit energy normalisation (UEN). However, the power gain can be greater than unity when the water-pouring formulas are used to calculate the capacity of ISI channels. In [1], a minimum $E_b/N_0$ of $-4.6$ dB was shown for the $1+D$ ISI channel, 3 dB below the capacity of a flat channel. The authors made the statement that "the ISI channel in this example is normalised with unit energy and thus does not provide any power gain by itself". This paper did not take into account that the channel power gain can be greater than unity for the $1+D$ ISI channel when using a water-pouring spectrum for the transmit power. Similar results were obtained for the $1-D$ Dicode channel in [2] and in [3] [4] where capacity was plotted against $E_s/N_0$.

In this paper, we examine the water-pouring capacity and channel normalisation of ISI channels. When water-pouring is used, the transmit power is not flat for a non-flat channel. Significant portions of the transmit power is concentrated near the peak of the channel frequency response. Since the maximum power gain is different for various ISI channels, it is not fair to compare the capacity of the unit energy normalised channel when the water-pouring formulas are used. We present a novel frequency response normalisation method which is physically meaningful and suitable for generic ISI channels. Compared to unit energy normalisation, our proposed channel normalisation method ensures no particular channel model has a gain over another one.

Wei Xiang is with the Institute for Telecommunications Research, University of South Australia, Mawson Lakes SA 5095, Australia. E-mail: wei@spri.levels.unisa.edu.au.

Steven S. Pietrobon is with the Institute for Telecommunications Research, University of South Australia, Mawson Lakes SA 5095, Australia. He is also with the Small World Communications, 6 First Avenue, Payneham South, SA 5070, Australia. E-mail: steven@sworld.com.au.

This work was carried out with financial support from the Commonwealth of Australia through the Cooperative Research Centres Program. The material in this paper will be presented in part at IEEE ICC2003, Anchorage, Alaska, USA, May 2003.

## II. Capacity

For a flat additive white Gaussian noise (AWGN) channel, it is well known that the capacity for this channel is

$$C = W \log_2 \left(1 + \frac{S}{N}\right), \tag{1}$$

where $C$ is the capacity in bit/s, $W$ is the bandwidth in Hz and $S/N$ is the signal to noise ratio.

For any channel that has a non-flat frequency response, we can use the water-pouring formulas to calculate its capacity. There is also another method for water-filling using the Kuhn-Tucker approach in [5]. According to the water-pouring theorem, the capacity at cost $S$ of a channel with noise spectrum $N(f)$ and input filter $H(f)$ is given in terms of a parameter $\theta$ [6]–[8]

$$C(S) = \frac{1}{2}\int_{-\infty}^{+\infty} \max\left[0,\ \log_2 \frac{\theta}{N(f)/\left|H(f)\right|^2}\right] df \tag{2}$$

$$S = \int_{-\infty}^{+\infty} \max\left[0,\ \theta - \frac{N(f)}{\left|H(f)\right|^2}\right] df, \tag{3}$$

where $C(S)$ is the capacity in bit/s and $S$ is the transmitted power in Watts. Fig. 1 illustrates the water-pouring formulas. The "water" poured into the shaded area is the transmit power $S$. Note that $|H(f)|^2$ represents the power gain with frequency for the channel. For an active channel this gain can be greater than unity, whereas it can be less than unity for a passive channel.

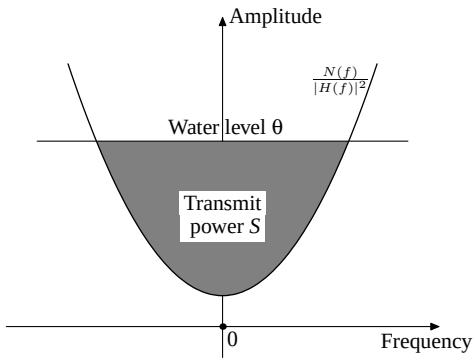


Fig. 1. Water-pouring illustration

The m-tap ISI channel is usually modelled as

$$y(k) = \sum_{i=0}^{m-1} h(i)x(k-i) + n(k), \tag{4}$$

where $x(k)$ is the channel input, $y(k)$ is the channel output, $n(k)$ is AWGN and the ISI channel is normalised using unit energy so that $\sum_{i=0}^{m-1} |h(i)|^2 = 1$.

For example, the spectrum of the 2-tap 1+D ISI channel is

$$H(f) = \begin{cases} \frac{1}{\sqrt{2}}\left[1 + e^{-j2\pi fT}\right] & ;-W \le f \le W \\ 0 & ;-W > f > W \end{cases} \tag{5}$$

where $T$ is the symbol period and with perfect Nyquist signaling $2WT = 1$. The AWGN spectrum is $N(f) = N_0/2$ Watt/Hz. For $|f| \le W$ we have $|H(f)|^2 = 1 + \cos(\pi f/W)$. The frequency responses of the 3-tap and 4-tap ISI channels are $|H(f)|^2 = ((1 + 2\cos(\pi f/W))^2/3$ and $|H(f)|^2 = 2\cos^2(\pi f/W) + 2\cos^3(\pi f/W)$, respectively. We plot the frequency responses of these three ISI channels in Fig. 2 with $W = 1$ Hz. Note that the peak of the frequency response is equal to $m$, the number of tap settings.

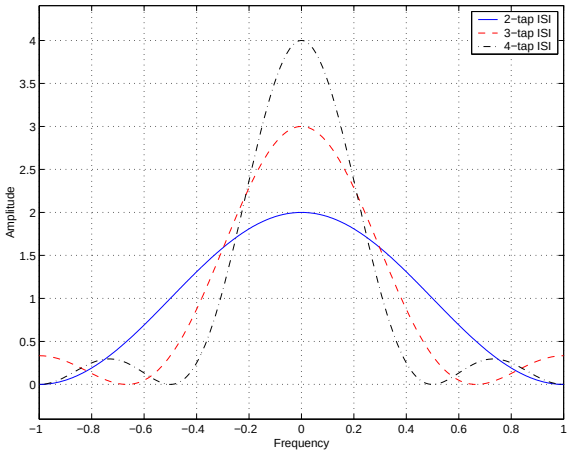


Fig. 2. Frequency response of three adder channels.

To determine the integration range for a given $\theta$, we let $\theta = N(w)/|H(w)|^2$, where $w$ are the "bowl" edges. For the $1 + D$ channel we have the edges at $-w$ and $w$ where

$$\theta = \frac{N_0/2}{1 + \cos(\pi f/W)}, \tag{6}$$

and (2) and (3) can be simplified into

$$C(S) = \frac{1}{2}\int_{-w}^{+w} \log_2\left[\frac{2\theta(1 + \cos(\pi f))}{N_0}\right] df \tag{7}$$

$$S = 2w\theta - \frac{N_0 W}{\pi}\tan\left(\frac{\pi w}{2W}\right). \tag{8}$$

For (7), the appropriate change of variables and the utilisation of [9, integrals 4.292.1 and 4.292.3] will yield closed form solutions for $\omega = 1/2$ and $\omega = 1$. For other values of $\omega$, numerical integration is used to plot the capacity curve. We have that the energy per bit at capacity is $E_b = S/C(S)$ and normalise $W$ to 1 Hz and $N_0$ to 1 W/Hz. We plot $C(S)$ versus $E_b/N_0$ in Fig. 3. Also plotted are the capacities of the 3-tap ISI, 4-tap ISI and flat AWGN channel. Note that the frequency responses of the three ISI channels are normalised with unit energy. As can be seen, the minimum $E_b/N_0$ for the 1+D channel is $-4.6$ dB, 3 dB below that of the flat channel of $-1.6$ dB. With a few more derivations, it can be shown that the minimum $E_b/N_0$ using water-pouring is $\ln(2)/|H(f_p)|^2$ where $f_p$ is the frequency at which $|H(f_p)|^2$ is maximum. For an m-tap adder channel, this gives a minimum $E_b/N_0$ of $\ln(2)/m$ when all the taps are equal.

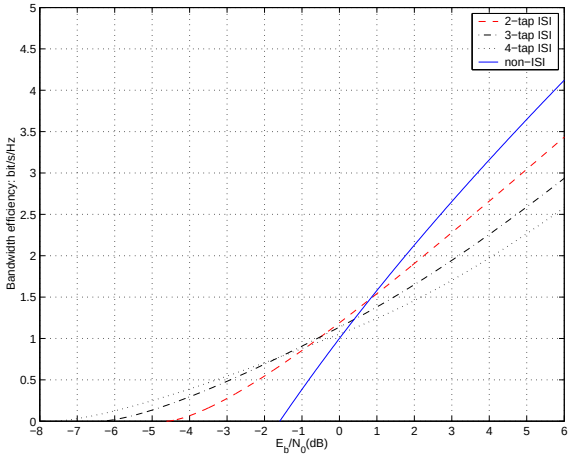


Fig. 3. Capacity of adder channels with unit energy normalisation.

For the $1 + D$ channel with unit energy normalisation, the maximum output to input power ratio is 2, although the average power gain over the whole frequency is 1. When the transmitter uses a water-pouring spectrum, a significant portion of the power is concentrated near the peak of the impulse response of the ISI channel. For the $1 + D$ channel, it is the maximum output to input power ratio of 2 that accounts for the 3 dB "gain" in the low-rate Shannon limit, relative to that of the flat channel with the unit energy frequency response.

The problem of conventional unit energy normalisation for ISI channels is that it neglects the fact that the maximum power gain can be greater than unity, and thus does not provide a fair capacity comparison for generic ISI channels. As can be shown, the minimum $E_b/N_0$ of an m-tap channel can be minus infinity when m goes up to infinity. Thus, it is not fair to compare the water-pouring capacity of a 2-tap channel with a maximum power gain of 2 with that of a 3-tap channel with a maximum power gain of 3. Therefore, a more well rounded power normalisation than unit energy normalisation is needed for the fair comparison of the capacities among generic ISI channels.

## III. Normalisation

A general communication system is depicted in Fig. 4. The transmit power $S_T$ is

$$S_T = \int_{-\infty}^{+\infty} \max\left[0,\ \theta - \frac{N(f)}{|H(f)|^2}\right] df, \tag{9}$$

The receive power $S_R$ is given by

$$S_R = \int_{-\infty}^{+\infty} \max\left[0,\ \theta\,|H(f)|^2 - N(f)\right] df, \tag{10}$$

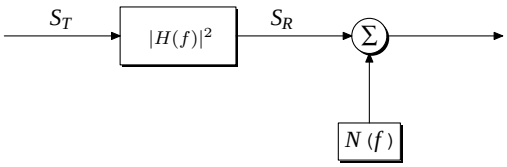


Fig. 4. Block diagram of ISI communications system

The channel power gain is defined as $S_R/S_T$. For a non-ISI channel or an ISI channel using a flat transmit power spectrum, the channel power gain is

$$\frac{S_R}{S_T} = \int_{-\infty}^{+\infty} |H(f)|^2 \, df, \tag{11}$$

which is usually normalised to unity.

However, for an ISI channel it is a function of $\theta$. One should be aware that the channel gain can be greater than unity in frequency ranges near the peak of the frequency response. One should therefore look only at $S_T$ as that allows us to determine total transmit power without having to worry about $\theta$.

When dealing with real channels, it is common to normalise the frequency response so that the maximum value is unity. Thus, we shall also normalise the power frequency to unity. This ensures that the minimum $E_b/N_0$ is always $-1.6$ dB.

The questions then remains as to what frequency normalisation to use. The technique should be applicable to finite bandwidth schemes such as m-tap ISI channel models and channel models with infinite bandwidths. For many non-flat channels, the "bandwidth" of the channel is usually given at the $-3$ dB (0.5) edges. We could also normalise the channel such that $\int_{-\infty}^{+\infty} |H(f)|^2 df = 2$. The former is simpler for channels with infinite bandwidths and the latter is simpler for m-tap ISI channels. Since our ultimate aim is to find capacities of real channels, we have chosen the former since it is more realistic. That is, we shall normalise the frequency response such that the $-3$ dB bandwidth is 1 Hz. We shall call this peak bandwidth normalisation (PBN).

Given the frequency response of an m-tap ISI channel with unit energy normalisation $|H(f)|^2$, the frequency response with peak bandwidth normalisation $|G(f)|^2$ is

$$|G(f)|^2 = \frac{1}{M} \left| H\left(\frac{f}{n}\right) \right|^2, \tag{12}$$

where $M$ is the maximum value of $|H(f)|^2$ and $n$ is the scaling factor which makes the $-3$ dB bandwidth of $|G(f)|^2$ equal to 1. Normalisation by the maximum value ensures the channel maximum power gain is unity. Thus, no particular channel has a gain over another channel in the frequency ranges where the transmit power is concentrated. Fig. 5 shows the frequency responses of the channels in Fig. 2 after applying the proposed peak bandwidth normalisation.

Note that if a flat transmit power spectrum is used we have $S_R/S_T = 1/M$ with peak bandwidth normalisation, where the transmit bandwidth is from -$n$ to $n$ Hz. This is not a fair comparison where flat transmit power is used. Thus, when using flat transmit power, the unit energy spectrum should be used to calculate the information rate of the channel. For water-pouring though, we believe the peak bandwidth spectrum is a more fair basis of comparison.

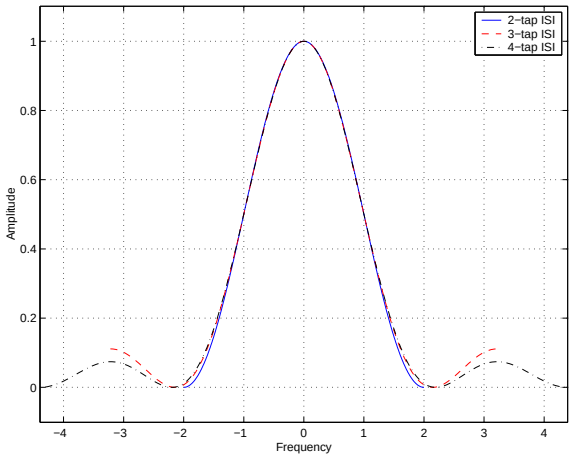


Fig. 5. Normalised frequency response of adder channels.

## IV. Numerical Results

In this section, we present numerical simulation results for the capacities of three types of ISI channels, namely the adder channels, RC channels and magnetic recording channels.

Fig. 6 showed the capacities of the three adder ISI channels, $C(S)$ in bit/s. We have $M = 2$, 3, and 4 and $n = 2$, 3.2201 and 4.3918 for the 2, 3, and 4-tap adder channels.

An important point to note in Fig. 5 is that at high $E_b/N_0$ the water-pouring capacity is greater than the flat channel capacity. This is directly due to the bandwidth expansion of the ISI channels at high $E_b/N_0$, even though for the $1 + D$ channel for example, $\int_{-\infty}^{+\infty} |G(f)|^2 df = 2$ is the same as for the flat channel. The transmit power after peak bandwidth normalisation $S'$ is

$$S' = \int_{-\infty}^{+\infty} \max\left[0, \; \theta - \frac{N(f)}{(1/M)|H(f/n)|^2}\right] df \tag{13}$$

$$= Mn \int_{-\infty}^{+\infty} \max\left[0, \; \frac{\theta}{M} - \frac{N_0/2}{|H(F)|^2}\right] dF, \tag{14}$$

where $F = f/n$ and $dF = (1/n)df$. The capacity power $C(S')$ after peak bandwidth normalisation is

$$C(S') = \int_{-\infty}^{+\infty} \max\left[0, \; \log_2 \frac{(\theta/M)|H(f/n)|^2}{N_0/2}\right] df \tag{15}$$

$$= n \int_{-\infty}^{+\infty} \max\left[0, \; \log_2 \frac{(\theta/M)|H(F)|^2}{N_0/2}\right] dF. \tag{16}$$

Dividing (14) by (16), we have

$$\frac{S'}{C(S')} = M \frac{S}{C(S)}. \tag{17}$$

Therefore, the curves in Fig. 6 are shifted by $M$ to the right from the curves in Fig. 3. However, the capacity $C(S')$ is increased by $n$. As shown later, when the actual bandwidth efficiency is taken into account, $C(S')/w' = C(S)/w$. That is, the ISI capacity is always below flat channel capacity.

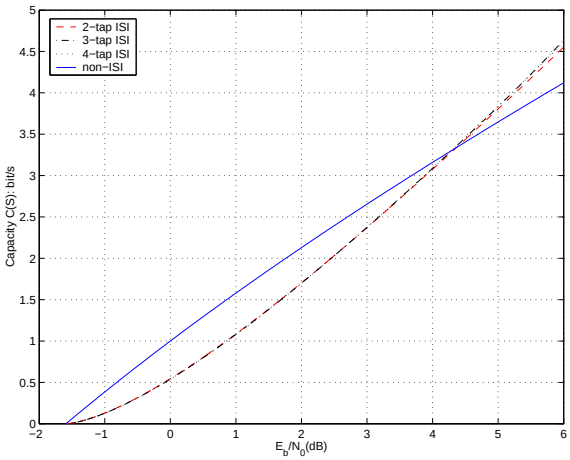


Fig. 6. Capacity in bit/s of adder channels.

The water-pouring capacities plotted in Fig. 3 assume that the bandwidth is equal to $W$ which is normalised to 1 Hz. However, if the transmitter uses the water-pouring spectrum, then we can normalise the capacity with the actual bandwidth used. In Fig. 7, we plot the bandwidth efficiency $C(S)/w$ (bit/s/Hz) where $w$ is the "bowl" edge. For 3-tap and 4-tap channels, the side lobes are not included for high SNR as bandwidth efficiency is reduced due to the large increase in bandwidth. That is, the maximum integration limits were set to -2.1467 to 2.1467 for the 3-tap peak bandwidth channel and -2.1959 to 2.1959 for the 4-tap peak bandwidth channel.

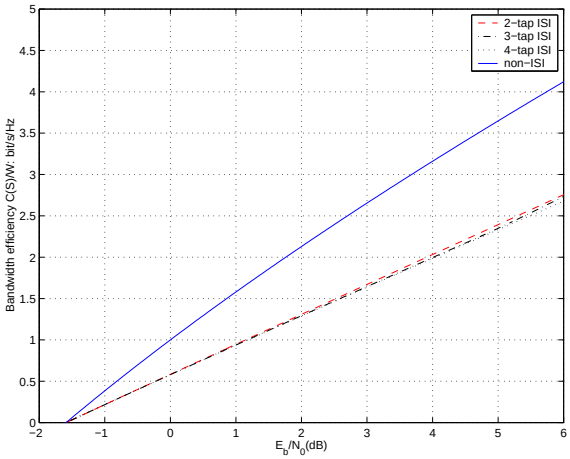


Fig. 7. Bandwidth efficiency in bit/s/Hz of adder channels.

Three types of RC channels were considered in this research, *i.e.*, the $1/(1+f^2)$ channel, the $1/(1+f^4)$ channel and the $1/(1+f^6)$ channel. The impulse responses of these channels are plotted in Fig. 8. Note that the $-3$ dB bandwidth is normalised to 1 Hz. The RC name comes from the fact that these channels can be modelled by resistor capacitor networks.

Figs. 9 and 10 show the capacity $C(S)$ in bit/s and the bandwidth efficiency in bit/s/Hz of the RC channels.

For RC channels, as the channel frequency spectrum becomes more square, the capacity approaches that of the flat channel.

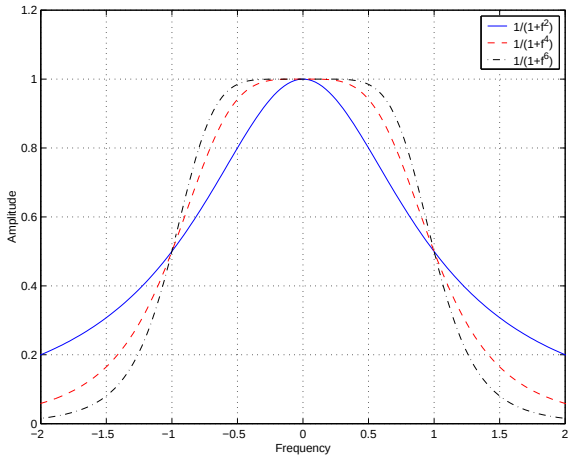


Fig. 8. Normalised frequency response of RC channels.

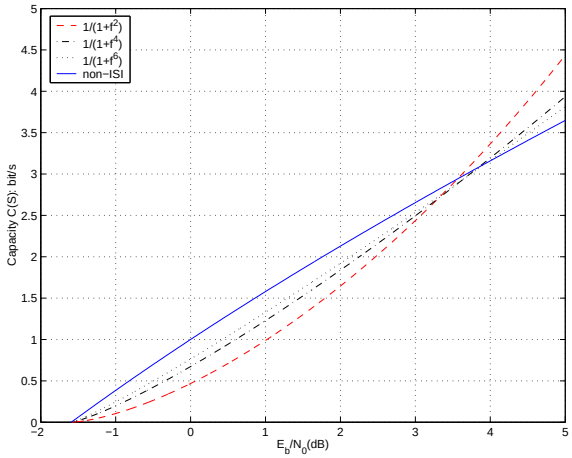


Fig. 9. Capacities C(S) in bit/s of RC channels.

Also considered are the Dicode $(1-D)$, PR4 $(1-D^2)$ and EPR4 $(1-D)(1+D^2)$ magnetic recording channel models. The unit energy frequency responses are $|H(f)|^2 = 2(1-\cos(\pi f/W))$, $2(1-\cos^2(\pi f/W))$, and $2(1-\cos(\pi f/W))(1+\cos^2(\pi f/W))$, respectively. For partial response channels, inputs are constrained to the set of $-1, 1$. The input can be spectrally shaped by using precoding. Since water-pouring assumes Gaussian inputs, the capacities in this paper are upper bounds to the binary input capacity. In [10], an expectation-maximization method was proposed to find tight lower bounds on the capacities of Markov sources over partial response channels.

Fig. 11 shows the frequency responses of the partial response (PR) channels with unit energy normalisation. Fig. 12 shows these frequency responses with peak bandwidth normalisation. We have $M = 2$, 2 and 2.3704 and $n = 2$, 2 and 2.3901 for the Dicode, PR4, and EPR4 channel models, respectively.

Fig 13 shows the capacity $C(S)$ in bit/s of the partial response channels using UEN. The Dicode and PR4 capacities are the same. However, the EPR4 capacity is quite different. The capacity and bandwidth efficiency of partial response

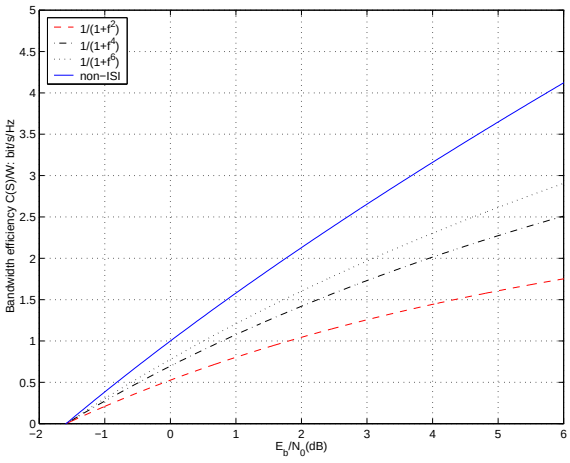


Fig. 10. Bandwidth efficiency C(S)/w in bit/s/Hz of RC channels.

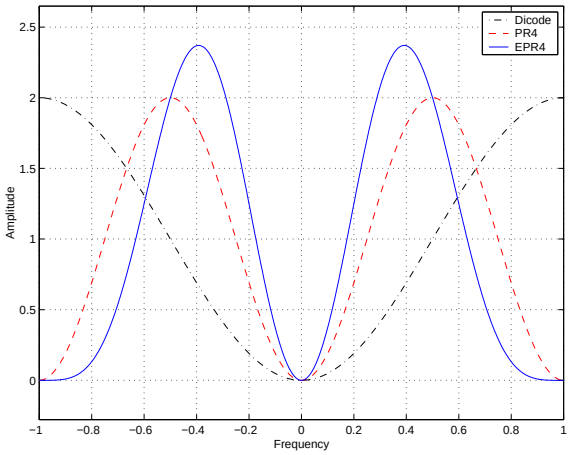


Fig. 11. Frequency response of PR channels.

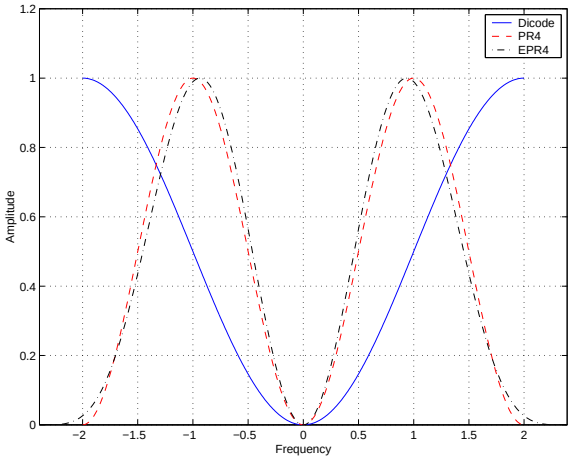


Fig. 12. Normalised frequency response of PR channels.

channels using PBN are shown in Figs. 14 and 15. One can notice both the capacity curves and bandwidth efficiency curves are very close to each other after applying the proposed power normalisation. We see that UEN gives different capacities for different channel models, whereas PBN gives similar capacities for different channel models. For instance, Dicode, PR4 and EPR4 are three different models of the same physical magnetic recording channel. We believe the three channel models should have similar capacities since they are modelled for the same physical channel. That is, PBN gives us similar capacities for the same physical channel, compared to UEN which can give quite different capacities for channel models of the same physical channel.

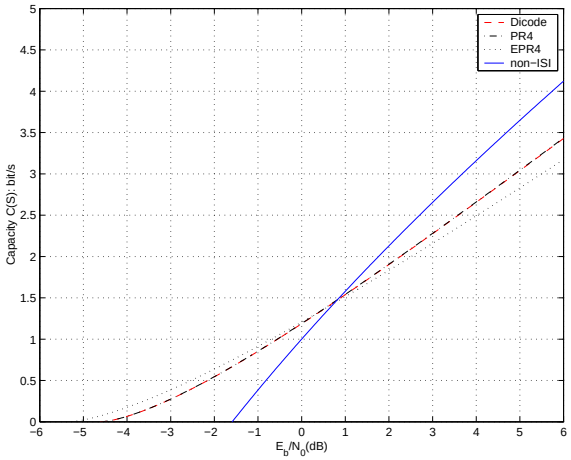


Fig. 13. Capacities C(S) in bit/s of PR channels using UEN.

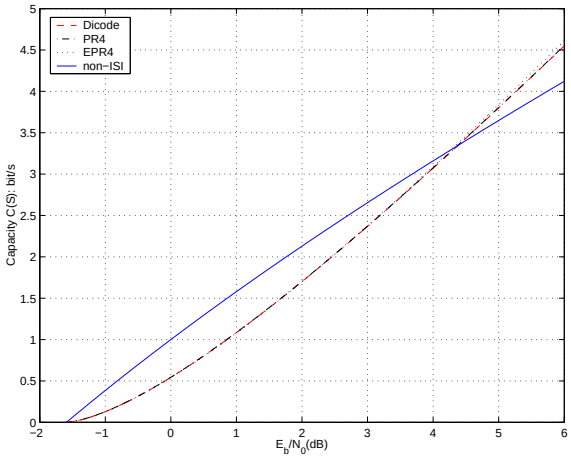


Fig. 14. Capacities C(S) in bit/s of PR channels using PBN.

## V. Conclusions

The unit energy normalised channel frequency response has an average power gain of unity over the whole bandwidth of the channel. That is not a problem when the frequency response is flat or the transmitter uses a flat power spectrum. However, the channel gain can be greater than unity when water-pouring is used to calculate the channel capacity.

With peak bandwidth normalisation proposed in this paper, the maximum channel power gain is normalised to 1 and the $-3$ dB (0.5) bandwidth of the channel frequency response is normalised to 1 Hz. Thus when water-pouring is performed, no particular ISI channel has a gain over another one. This normalisation can be used as a criterion of fair capacity comparison among generic ISI channels.

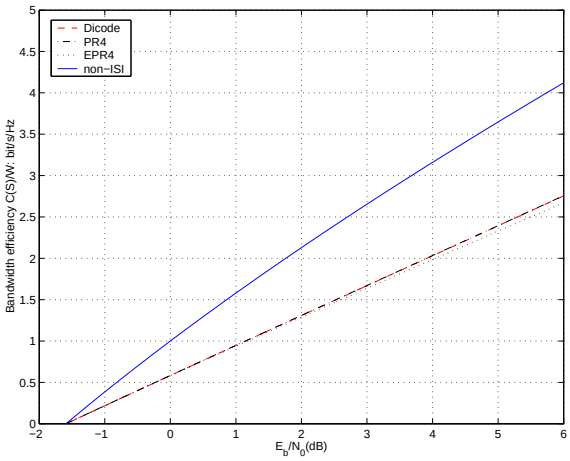


Fig. 15. Bandwidth efficiency C(S)/w in bit/s/Hz of PR channels using PBN.

## ACKNOWLEDGMENTS

The authors would like to thank Dr. Alex Grant and Prof. Paul Siegel for their discussions and comments.

## REFERENCES

[1] Y.-J. A. Zhang and X.-G. Xia, "Joint turbo and modulated code encoding decoding for ISI channels," in *Proc. IEEE Int. Symp. Inform. Theory*, Washington, DC, USA, p. 266, June 2001.

[2] H. D. Pfister, J. B. Soriaga, and P.H. Siegel, "On the achievable information rates of finite state ISI channels," in *Proc. GLOBECOM 2001*, vol. 5, San Antonio, TX, USA, Nov. 2001, pp. 2992 -2996.

[3] D. Arnold and H. Loeliger, "On the information rate of binary-input channels with memory," in *Proc. IEEE Int. Conf. Commun.*, vol.9, pp. 2692-2695, Helsinki, Finland, June 2001.

[4] P. O. Vontobel and D. M. Arnold, "An upper bound on the capacity of channels with memory and constraint input," in *Proc. IEEE Inform. Theory Workshop*, pp. 147-149, Cairns, Australia, Sept. 2001.

[5] T. M. Cover and J. A. Thomas, *Elements of Information Theory*. New York: Wiley, 1991.

[6] R. M. Gray, "On the asymptotic eigenvalue distribution of Toeplitz matrices," *IEEE Trans. Inf. Theory*, vol. IT-18, pp. 725-730, Nov. 1972.

[7] B. S. Tsybakov, "On the transmission capacity of a discrete-time Gaussian channel with filter," *Prob. Peredachi Informatzii*, pp. 78-82, 1970.

[8] R. E. Blahut, *Principles and Practice of Information Theory*. Massachusetts: Addison-Wesley, 1987.

[9] I. S. Gradshteyn and I. M. Ryzhik, *Table of Integrals, Series, and Products*. New York: Academic Press, 1980.

[10] A. Kavcic, "On the capacity of Markov sources over noisy channels," in *Proc. GLOBECOM 2001*, vol. 5, San Antonio, TX, USA, Nov. 2001, pp. 2997-3001.

**Wei Xiang (S'01)** was born in Jingdezhen, China in 1975. He received the B.Eng. and M.Eng. degrees in electronic engineering from the University of Electronic Science and Technology of China in 1997 and 2000, respectively. In July 2000, he was awarded an international postgraduate research scholarship to study towards a Ph.D. degree in the Institute for Telecommunications Research, University of South Australia. He is currently a member of Cooperative Research Centre for Satellite Systems (CRCSS).

His research interests include joint source-channel coding and decoding, wireless multimedia communications and error control coding.

**Steven S. Pietrobon** Dr. Pietrobon was born in Naracoorte, South Australia on 5 October 1963. He received the B.Eng. and M.Eng. degrees in electronic engineering from the South Australian Institute of Technology (SAIT, now University of South Australia), Adelaide, South Australia in 1986 and 1989, respectively, and the Ph.D. degree in electrical engineering from the University of Notre Dame, Notre Dame, Indiana, U.S.A., in 1991. He received a SAIT Medal for outstanding academic achievement for his B.Eng. degree.

In 1991 he joined the Australian Space Centre for Signal Processing, University of South Australia as a Research Fellow. In 1993 he was awarded a three year Australian Postdoctoral Research Fellowship at the University of South Australia. In 1997 he started his own business "Small World Communications" developing error control decoders for programmable gate arrays. Dr. Pietrobon also became Adjunct Research Fellow at the Institute for Telecommunications Research, University of South Australia in 1997. In 2000 he was promoted to Adjunct Senior Research Fellow. From 1996-1999 he was a Coding Theory and Techniques Editor for the IEEE Transactions on Communications. He is currently a member of the organising committee of the IEEE 2004 International Symposium on Spread Spectrum Techniques and Applications. His research interests include convolutional, trellis, and turbo coding and implementation of Viterbi, trellis, MAP, and turbo decoders.